


















ARTICLE

Growth portfolios buffer climate-linked environmental change in marine systems

Steven E. Campana¹  | Szymon Smoliński^{2,3}  | Bryan A. Black⁴  |
 John R. Morrongiello⁵  | Stella J. Alexandroff⁶ | Carin Andersson⁷  |
 Bjarte Bogstad²  | Paul G. Butler⁶  | Côme Denechaud^{2,8}  |
 David C. Frank⁴  | Audrey J. Geffen⁸  | Jane Aanestad Godiksen²  |
 Peter Grønkjær⁹  | Einar Hjörleifsson¹⁰ | Ingibjörg G. Jónsdóttir¹⁰  |
 Mark Meekan¹¹  | Madelyn Mette¹²  | Susanne E. Tanner¹³  |
 Peter van der Sleen¹⁴ | Gotje von Leesen^{1,9} 

¹Life and Environmental Sciences, University of Iceland, Reykjavik, Iceland

²Institute of Marine Research, Bergen, Norway

³National Marine Fisheries Research Institute, Gdynia, Poland

⁴Laboratory of Tree-Ring Research, University of Arizona, Tuscon, Arizona, USA

⁵School of BioSciences, University of Melbourne, Melbourne, Victoria, Australia

⁶Centre for Geography and Environmental Sciences, University of Exeter, Penryn, UK

⁷NORCE Norwegian Research Centre, Bjerknes Centre for Climate Research, Bergen, Norway

⁸Department of Biological Sciences, University of Bergen, Bergen, Norway

⁹Aquatic Biology, Department of Biology, Aarhus University, Aarhus, Denmark

¹⁰Marine and Freshwater Research Institute, Reykjavik, Iceland

¹¹Australian Institute of Marine Science, Perth, Western Australia, Australia

¹²U.S. Geological Survey, St. Petersburg Coastal and Marine Science Center, St. Petersburg, Florida, USA

¹³Marine and Environmental Sciences Centre and Department of Animal Biology, Faculty of Sciences, University of Lisbon, Lisbon, Portugal

¹⁴Wildlife Ecology and Conservation Group and Forest Ecology and Management Group, Wageningen University and Research Centre, Wageningen, The Netherlands

Correspondence

Steven E. Campana

Email: scampana@hi.is

Funding information

Australian Research Council,

Grant/Award Number: DP190101627;

Eimskip University Fund, Grant/Award

Number: 1535-1533127; Fundação para a

Ciência e a Tecnologia, Grant/Award

Number: CEECIND/02710/2021;

Abstract

Large-scale, climate-induced synchrony in the productivity of fish populations is becoming more pronounced in the world's oceans. As synchrony increases, a population's "portfolio" of responses can be diminished, in turn reducing its resilience to strong perturbation. Here we argue that the costs and benefits of trait synchronization, such as the expression of growth rate, are context dependent. Contrary to prevailing views, synchrony among individuals could actually be beneficial for populations if growth synchrony increases during

This is an open access article under the terms of the [Creative Commons Attribution-NonCommercial-NoDerivs](https://creativecommons.org/licenses/by-nc-nd/4.0/) License, which permits use and distribution in any medium, provided the original work is properly cited, the use is non-commercial and no modifications or adaptations are made.

© 2022 The Authors. *Ecology* published by Wiley Periodicals LLC on behalf of The Ecological Society of America.

Havforskningsinstituttet, Grant/Award Number: 14260; Icelandic Centre for Research, Grant/Award Number: 173906-051; Nordisk Ministerråd, Grant/Award Number: 25014.17; Norges Forskningsråd, Grant/Award Number: 240550; Australian Academy of Science's Thomas Davies Research; University of Bergen

Handling Editor: Daniel E. Schindler

favorable conditions, and then declines under poor conditions when a broader portfolio of responses could be useful. Importantly, growth synchrony among individuals within populations has seldom been measured, despite well-documented evidence of synchrony across populations. Here, we used century-scale time series of annual otolith growth to test for changes in growth synchronization among individuals within multiple populations of a marine keystone species (Atlantic cod, *Gadus morhua*). On the basis of 74,662 annual growth increments recorded in 13,749 otoliths, we detected a rising conformity in long-term growth rates within five northeast Atlantic cod populations in response to both favorable growth conditions and a large-scale, multidecadal mode of climate variability similar to the East Atlantic Pattern. The within-population synchrony was distinct from the across-population synchrony commonly reported for large-scale environmental drivers. Climate-linked, among-individual growth synchrony was also identified in other Northeast Atlantic pelagic, deep-sea and bivalve species. We hypothesize that growth synchrony in good years and growth asynchrony in poorer years reflects adaptive trait optimization and bet hedging, respectively, that could confer an unexpected, but pervasive and stabilizing, impact on marine population productivity in response to large-scale environmental change.

KEYWORDS

climate, ecological buffer, fish populations, growth synchrony, otolith, productivity, stabilization

INTRODUCTION

Large-scale climate processes play a critical role in shaping patterns of biological productivity, with phenomena such as the El Niño–Southern Oscillation (ENSO) and the North Atlantic Oscillation (NAO) ultimately driving growth, recruitment and migration patterns in marine ecosystems (Stenseth et al., 2002). The spatial scale of these climate phenomena is sufficiently large to cause synchronous impacts on the demography of multiple populations (the “Moran effect”) (Black et al., 2018; Liebhold et al., 2004). In the event of a climatic extreme that causes extensive mortality, a synchronous response could leave no unaffected populations available for restocking, potentially leading to extirpation.

The Moran effect is typically assessed in terms of population abundance, which in turn is regulated through the processes of mortality and fecundity. Yet somatic growth rate can also influence population abundance in fishes, since reproduction and mortality rate are inextricably linked to individual growth through size- and density-dependent processes (Beverton & Holt, 1957). Indeed, plasticity in growth rate is a universal feature of animal life histories, and is strongly correlated to both mortality and fitness (Dmitriew, 2011).

Importantly, growth synchrony among individuals (Figure 1) has seldom been measured within populations.

We hypothesize that unsynchronized growth among individuals in poor years may diversify growth and subsequent maturation portfolios, thus increasing the resilience of a population to environmental perturbations, whereas synchronized growth resulting from good years could allow more individuals to experience maximal growth and thus fitness. Our hypothesis differs from the standard interpretation of portfolio theory, whereby individuals (or populations) with different traits respond uniquely to the same changes in environmental conditions, resulting in good years for some individuals and bad years for others. We argue that individuals should synchronize their growth during fast-growing years (to capitalize on favorable conditions) and asynchronize their growth during slow-growing years (bet-hedging). If there was an influence of large-scale, low-frequency climate phenomena on among-individual traits operating at small scales and over short time periods (such as growth synchrony), shifts in climate modes and phases could affect the stability and productivity of populations in a manner not previously suspected. Here, we exploit the long-term individual-based growth histories naturally archived in the calcified otoliths (earstones) of an

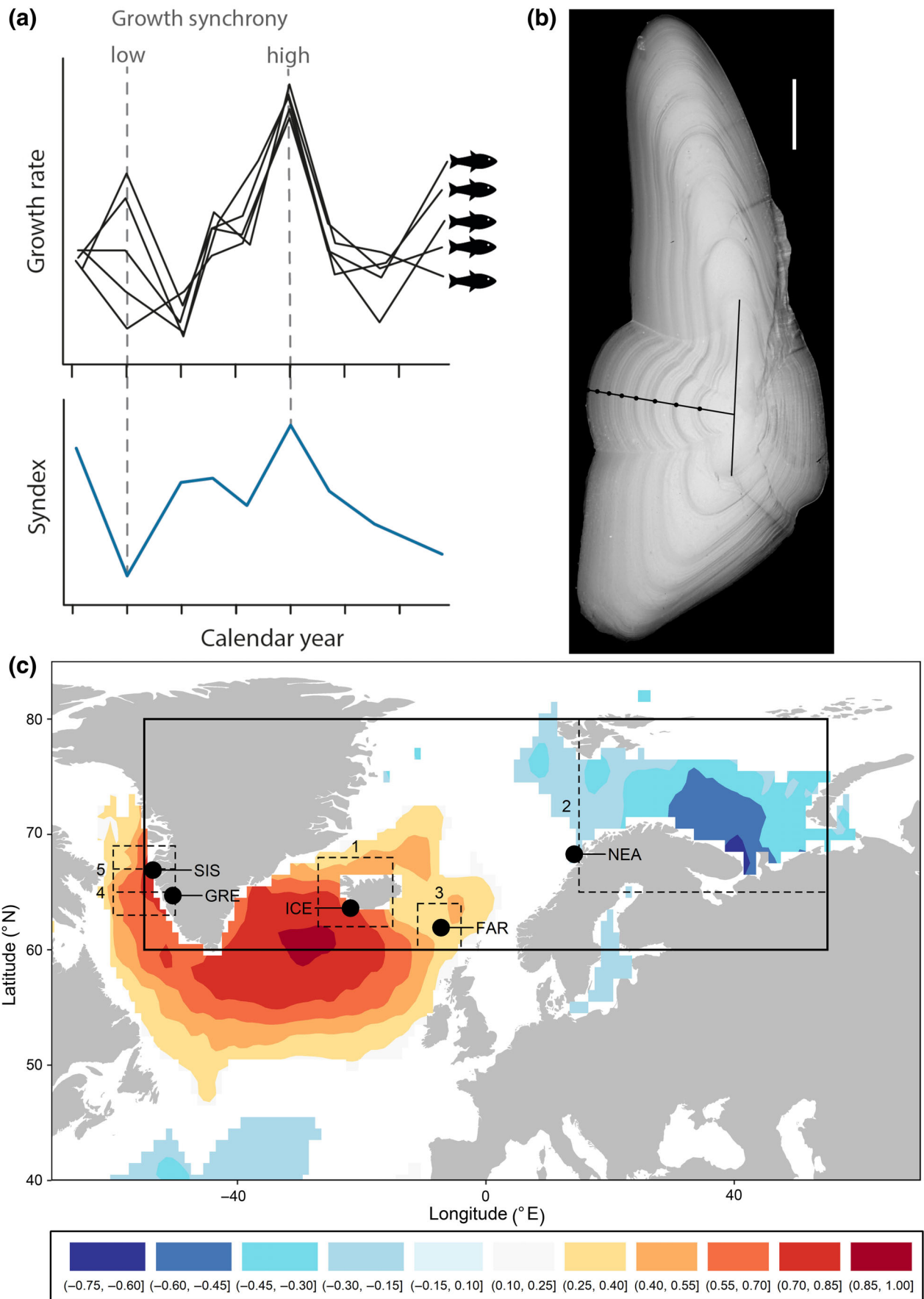


FIGURE 1 Legend on next page.

intensely monitored marine fish species to empirically test how local demography and large-scale climatic phenomena affect the expression of among-individual growth synchrony across the Northeast Atlantic.

METHODS

Cohort-specific growth synchrony has seldom been examined in any animal species, leaving open the question of its cause and its ubiquity across the animal kingdom. Our analysis was first directed to environmental or biological factors that might conceivably influence growth and its synchrony in Atlantic cod (such as temperature, food supply, and density-dependence) before moving onto possible causes. We complement these analyses with further insight drawn using published and unpublished growth chronologies from other fish species, bivalves, and trees.

Cod otolith sampling

Growth chronologies were based on cod sampled at annual intervals over periods of up to 94 years from five major cod populations in the Northeast Atlantic (Appendix S1: Table S1). For the migratory populations of Norway and Iceland, samples were collected from the main spawning grounds during the spawning season (Norway: the Lofoten archipelago, January–early May; southwestern Iceland: March–May). The Faroe cod population was sampled on the Faroe plateau spawning grounds during the spawning season (February–April) at bottom depths shallower than 150 m. The Godthaabsfjord cod population on the west coast of Greenland (64° N, 51° W, NAFO Division 1D) was sampled mainly (88%) between April and September, with small numbers caught during the remainder of the year. Cod from the inshore area around Sisimiut, West Greenland (66°45' N, 53°30' W, NAFO Division 1B) were primarily caught during June to August (70%), whereas the rest were caught during April, May, September and October. Most samples were collected with research or commercial bottom trawls, supplemented by commercial longlines, jigs, and pound nets. Otoliths from the above samples were subsequently

retrieved from archives at the Faroese Marine Research Institute (Faroe Islands), Greenland Institute for Natural Resources (Greenland), Marine and Freshwater Research Institute (Iceland), and Institute of Marine Research (Norway). Due to a probable size-selectivity bias, otoliths from fish caught using gillnets were excluded from the Icelandic and Norwegian selection (Denechaud et al., 2020; Smoliński, Deplanque-Lasserre, et al., 2020).

In order to robustly estimate growth variation across growth years and annual fish cohorts, large sample sizes from multiple overlapping cohorts are required (Morrongiello, Bond, et al., 2012; Morrongiello, Thresher, & Smith, 2012; Smoliński, Morrongiello, et al., 2020). Wherever possible, samples for the Icelandic and Northeast Arctic (NEA) cod populations consisted of at least 50 otoliths per year from mature fish (age 8 or older), although the sampling target was 30 otoliths per year for the Faroese (ages 5–6), Godthaabsfjord (ages 5–6), and Sisimiut (ages 4–10) populations. The cod aging method is known to be both accurate and precise (CV < 3.8%) (Campana, 2001; Smoliński, Deplanque-Lasserre, et al., 2020).

Otolith growth chronologies

Otolith growth chronologies were constructed from series of annual increment widths measured from digitized images of sectioned otoliths. Since the date and age at capture (corresponding to the otolith margin) was known, each increment could be assigned a year and age of formation. Norwegian, Icelandic, and Faroese (1980–1990 only) otoliths were embedded in epoxy and sectioned transversely through the core (Denechaud et al., 2020; Smoliński, Deplanque-Lasserre, et al., 2020). The Godthaabsfjord, Sisimiut, and post-1990 Faroese otoliths were sectioned without embedding and subsequently heat-treated to increase the contrast between opaque and translucent zones (Christensen, 1964). All images were captured under reflected light using high-resolution image analysis systems. Increment widths (μm) were measured along an axis drawn from the otolith core to the distal edge, thus intersecting the maximum number of annual increments at a perpendicular angle (Figure 1b). In Norway and Iceland, because the position of the core was not always clear, the longest diameter of the first

FIGURE 1 (a) Conceptual framework of the fish growth synchrony index (Syndex). (b) Transverse section of the otolith of an 8-year old cod (*Gadus morhua*), viewed under reflected light. The horizontal line identifies the axis along which annual growth increments (marked by dots) were measured. The vertical line identifies the first year of growth. Scale bar = 1 mm. (c) Map of North Atlantic Ocean showing the polygon (solid black line) used to define the second empirical orthogonal function (EOF-2) of sea surface temperature (SST) over the study area. Correlation between EOF-2 and SST is indicated with a color gradient. SST regions for individual cod stocks (dashed polygons) also indicate cod sampling locations (solid circles). FAR, Faroese; GRE, Godthaabsfjord; ICE, Iceland; NEA, Northeast Arctic; SIS, Sisimiut.

increment was marked and the intersection point between the diameter and the measuring axis was used as the origin for the measurements (Denechaud et al., 2020). Because of this difference, the width of the innermost increment was not included in the analysis of the Icelandic samples. Annual increments were measured as the width of a translucent and opaque zone pair: from the medial edge (distal edge in the case of Iceland and NEA) of the opaque zone to the end of the subsequent translucent zone, and were measured across the entire growth sequence of each otolith. Here, the data analysis was restricted to increments formed at ages 1–6, since these ages were represented in all populations and most fish were still sexually immature. Thus inter-annual growth fluctuations most likely reflected environmental conditions and/ or the effects of density-dependent competition for resources rather than the energetic costs of reproduction. A total of 13,749 otoliths and 74,662 annual increments were measured in this study. Data are available at Campana (2022a).

Additional fish chronologies

Otoliths from 671 female plaice (*Pleuronectes platessa*) individuals were sampled over roughly the region 4–8° E, 55–57° N during a Beam Trawl Survey (BTS-Solea) in the month of August over the period 1993–2015, which provided growth-increment data from 1985 to 2014 (van der Sleen et al., 2018). Only female plaice were selected because of better reading clarity, and because of the much higher availability of female samples (of the >700 samples only 30 were from males).

Otoliths from Atlantic horse mackerel (*Trachurus trachurus*) and European hake (*Merluccius merluccius*) were obtained from market sampling and research surveys carried out by the Portuguese Institute for the Sea and Atmosphere along the Portuguese coast (8–10° W, 37–42° N) from 1975 (horse mackerel)/1979 (hake) to 2016. For both species, otoliths were selected ensuring a balanced sex ratio and covering all fish sizes available per capture year and location. Atlantic horse mackerel otoliths ($n = 2918$) provided growth-increment data from 1963 to 2015 (Tanner et al., 2019) and European hake otoliths ($n = 1869$) produced a growth-increment chronology spanning from 1973 to 2015 (Vieira et al., 2020).

Samples of the two deep-sea scorpaenid fish species (blackbelly rosefish, *Helicolenus dactylopterus* and offshore rockfish *Pontinus kuhlii*) were obtained from fisheries-independent research cruises carried out by the Department of Oceanography and Fisheries of the University of the Azores from 1996 to 2017. Only otoliths of individuals captured in the central island group of the

Azores archipelago (27.5–29° W, 38–39° N) were selected. Blackbelly rosefish otoliths ($n = 337$) provided 4887 growth increment widths from 1971 to 2016 and 472 otoliths of offshore rockfish resulted in 5690 growth increment widths covering the period from 1972 to 2016 (Tanner et al., 2020).

Bivalve growth chronologies

Shells from the marine bivalve, *Arctica islandica*, were collected from a 0.5 km² area at Ingøya, Norway (71°03.734' N, 24°05.895' E; ~10 m water depth) between June 2009 and June 2015 (Mette et al., 2021) and from Faxaflói, southwest Iceland (64°21.960' N, 23°7.046' W, ~102 m water depth) in July 2015 and August 2016. Shells were sectioned along the maximum growth axis and embedded in clear epoxy. Acetate replica peels of the shell cross sections were produced to examine and measure growth increments under transmitted light microscopy. Growth chronologies were constructed from 39 Norwegian individuals ranging in age from 128 to >390 years and 29 Icelandic individuals ranging in age from 35 to >400 years. Growth increments were imaged, measured, and visually crossdated along the outer shell margin and/or hinge plate along the maximum growth axis. Measurement series for the Norway and Icelandic shell growth chronologies were treated with trimming of the first 40 and at least the first 2 juvenile increments, respectively, and removing the ontogenetic growth trend (detrrending using modified negative exponential functions) (Mette et al., 2021). Standard chronologies were computed using the software package ARSTAN v44 (Cook et al., 2017) and then scaled to have zero mean and a standard deviation (SD) of 1. Annual growth increments were sampled for oxygen isotope analysis (Mette et al., 2021) and translated into temperature estimates using the aragonite-temperature equation (Grossman & Ku, 1986), as modified by (Dettman et al., 1999): $T (^{\circ}\text{C}) = 20.60 - 4.34 \times (\delta^{18}\text{O}_{\text{shell}} - [\delta^{18}\text{O}_{\text{water}} - 0.27])$.

Cod abundance chronologies

The stock dynamics of Icelandic cod is well documented for the period after 1955 (Schopka, 1994), and somewhat less so for the early years (Hansen et al., 1935). A single consistent time series was prepared by combining the catch-at-age (age 3–14) matrix for the years 1928–1954 (Schopka, 1994) with the 1955 to 2017 catch at age compilation as published in the ICES NWWG 2018 report: ICES (2019): North-Western Working Group (NWWG). The statistical catch-at-age assessment model assumed constant

selectivity for each of six periods (years 1928–1937, 1938–1949, 1950–1975, 1976–1993, 1994–2003, 2004–2017). Tuning indices were based on age groups 1 to 10 from the Icelandic spring groundfish survey and Icelandic autumn groundfish survey (Schopka, 1994). Natural mortality was scaled to 0.2 for all age groups, the catch weights at age were used to estimate the reference biomass of ages 4 and above, and the survey weights and maturity at age from the spring survey were used to estimate the spawning stock biomass. Prior to 1985, spawning weights were based on a regression of the survey and catch weights for the period after 1985. Full maturity and a spawning migration were assumed at ages ≥ 6 prior to 1928.

Sporadic immigration of adult cod from Greenland into Icelandic waters is known to occur. The number of immigrants was estimated for the following years and ages: 1930–8, 1933–9, 1953–8, 1958–9, 1959–9, 1960–10, 1962–9, 1964–10, 1969–8, 1970–8, 1972–9, 1980–7, 1981–8, 1990–6 and 2009–6. The estimates of the year and age of immigration after 1955 were the same as those reported in (Schopka, 1994), while the three immigration events prior to 1955 were only estimated for very abundant cohorts (1922, 1924, and 1945); the year and age of the immigration events were based on anomalies in the catch at age structure, and by tagging studies for the 1922 and 1924 events (Hansen et al., 1935).

Time series of population numbers, fishing mortalities, total stock biomass, and spawning stock biomass were available for Northeast Arctic cod for ages 3–15+ since 1930. The time series were based on a Virtual Population Analysis (VPA) for the years 1930–1945 (Hysten, 2002), and the ICES stock assessment for 1946–2020 (ICES AFWG, 2020a). To the extent possible, the two assessment time series were made consistent (Rørвик et al., 2022).

Abundance-at-age data for the Faroese cod were based on a State-space Assessment Model (SAM) tuned using annual groundfish surveys carried out since 1982 (ICES NWWG, 2020b; Kristiansen, 1988). Abundance data were not available for the Greenland populations.

Absolute abundance varied by several orders of magnitude among the five cod populations. To test for the effects of cod density on growth synchrony, cod absolute abundance at age was standardized across populations by normalizing to the largest observed abundance at age within each population, and thus can be considered as an index of some proportion of carrying capacity for that population (assuming that carrying capacity is stable across years, which it is not). This approach was used for the century-scale time series of both the Icelandic and Northeast Arctic cod populations but was not suitable for the much shorter (1959–2018) Faroes population time series. Assuming that 1959–1960 were the years with the

lowest Faroese fishing mortality (and thus the highest abundance) and given that Icelandic and Faroese annual abundance at age were significantly correlated ($p < 0.05$), and since the period 1959–1960 was 61% of the Icelandic maximum since 1928, the Faroese abundance at age estimates were similarly assumed to represent 61% of their maximum values in 1959–1960.

Temperature and climate data

Sea surface temperature (SST) was the only measure of water temperature that was available for the entire study area and time period and is a good reflection of broad climate trends. An empirical orthogonal function (EOF) of SST explaining 61% of the variance (45.1% of the variance for EOF1 and 16.1% of the variance for EOF2) was calculated using the mean annual May through October sea surface temperature (SST) within the region -55° to 55° E and 60° to 80° N. The analysis was performed for the time period 1870–2020 using the 1° gridded Hadley ISST dataset (Rayner et al., 2003) in the KNMI Climate Explorer (Trouet & van Oldenborgh, 2013; von Leesen et al., 2020). Mean May through October Hadley ISST was also averaged within each of the cod stock polygons bounded by: Godthaabsfjord ($50-60^\circ$ W, $63-67^\circ$ N), Sisimiut ($50-60^\circ$ W, $65-69^\circ$ N), Iceland ($15-27^\circ$ W, $62-68^\circ$ N), Faroes ($4-11^\circ$ W, $60-64^\circ$ N), Northeast Arctic ($15-55^\circ$ E, $65-80^\circ$ N). Data sets utilized for this research are in Campana (2022a).

Mean SST varied substantially across the regions occupied by the cod populations, but within-region growth differences would be expected to be better reflected by within-region temperature anomalies. Thus, SST was decomposed into spatial and temporal components, with region-specific long-term mean temperatures used to quantify persistent spatial differences, and within-region temperature anomalies used to quantify local temporal variability of temperature. We calculated the average within-region temperature \bar{X}_{SST} , then the anomaly of temperature from this mean ($X_{SST} - \bar{X}_{SST}$). Anomalies were scaled within regions. The SST term used in the synchrony modeling was thus the within-region temperature anomaly.

Annual water temperatures at depth (200 m) were estimated for each age group within each cod population, using either observed or modeled subsurface temperature data, weighted by a maturity-at-age ogive and the proportion of the year spent on spawning grounds away from the feeding grounds. Greenlandic and Faroese cod do not migrate to spawn, thus a common temperature time series was estimated for all age classes. To properly weight the contributions from stations with variable

coverage across depth, time, and space, GLM were used to estimate the annual population-specific temperature time series, with month, year, depth and station as factors (von Leesen et al., 2022). Monthly Greenland water temperatures were available for depths ranging from 50 to 200 m, but were missing for the period 1987–2004. Faroese water temperatures were based on monthly bottom water temperatures on the Faroese shelf, with missing data interpolated using SST data, except in July to September, when depth stratification was pronounced. Any remaining missing values were interpolated using a fifth order polynomial. The temperature for NEA cod was based on observed water temperatures on the Kola section (0–200 m) covering the feeding grounds and from the Eggum and Skrova oceanographic stations near the Lofoten spawning area (von Leesen et al., 2020).

Zooplankton (CPR) chronologies

Zooplankton abundance data were obtained from the Continuous Plankton Recorder (CPR) Survey (Warner & Hays, 1994), covering the North Atlantic region (50° N–70° N) over the period 1959–2018 (Helaouet, 2020). We considered the abundance of *Acartia* spp., *Calanus* spp. (stages 1–4), *Calanus finmarchicus*, *Calanus helgolandicus*, large copepods, and small copepods (Beaugrand et al., 2003). We fitted generalized additive models (Wood, 2003) (GAM) for each group with the following formula:

$$y_{ijkl} = \alpha_i + f_1(x_j) + f_2(x_k, x_l) + \varepsilon_{ijkl}$$

$$\varepsilon_{ijkl} \sim N(0, \sigma^2)$$

where y_{ijkl} is zooplankton group abundance in year i , month j , at longitude k and latitude l , α is an intercept for each year i , f_1 is a cyclic cubic regression spline for the month j , f_2 is a tensor product splines for longitude k , and latitude l (Wood, 2001). This approach accounts for interannual, seasonal, and spatial variability in zooplankton abundance. We extracted year-effect estimates from the models as an indicator of interannual changes in abundance of zooplankton groups in the North Atlantic, which may influence cod growth and its synchrony (Beaugrand & Kirby, 2010). The GAM analysis was conducted in *R* (R Core Team, 2020) using the *mgcv* package (Wood, 2001), with all parameters set to default and using 12 knots for the cyclic cubic spline of the month effect. Since the zooplankton variable did not enter significantly into the Syndex model, it was not pursued further.

Base growth model development

We applied linear mixed-effect models to characterize variation in fish growth (Morrongiello & Thresher, 2015; Weisberg et al., 2010). Prior to the modeling, we log-transformed otolith annual increment width and age of fish (Appendix S1: Figure S7). After a series of model comparisons using Akaike’s Information Criterion corrected for the small sample size (AIC_c) we selected the following model structure:

$$y_{ijklmn} = \alpha_l + \alpha_i^F + \alpha_{klm}^Y + \alpha_{ln}^C + \beta_{jl}x_{jl} + b_{ij}^F x_{ij} + \varepsilon_{ijklmn}$$

$$\begin{bmatrix} \alpha_i^F \\ b_{ij}^F \end{bmatrix} \sim N\left(0, \sum_i\right), \quad \alpha_{klm}^Y \sim N(0, \sigma^2),$$

$$\alpha_{ln}^C \sim N(0, \sigma^2), \quad \varepsilon_{ijklmn} \sim N(0, \sigma^2).$$

where y_{ijklmn} , otolith annual increment width y for fish i at age j from age group k , population l , year m , and cohort n , α_l is the overall intercept for population l , α_i^F is the random intercept for fish i , α_{klm}^Y is the random extrinsic environmental effect for age group k from population l at year m , α_{ln}^C is the random intercept for population l and cohort n , $\beta_{jl}x_{jl}$ is the age-dependent (j) decline in growth specific to each population l , $b_{ij}^F x_{ij}$ is the random age (j) slope for fish i . The Age effect accounted for the decline in growth as fish aged, the form of which was assumed to be specific for each population. Random fish effects accounted for repeated measurements and specific differences in the growth of individuals. Random year effects accounted for the correlation of increments formed in the same year within the age group and population and can be associated with the combined environmental conditions affecting fish growth (Smoliński, Deplanque-Lasserre, et al., 2020). Random cohort effects accounted for the correlation of increments formed by fish from the same population that hatched in the same year (Appendix S1: Figure S8). We extracted both year and cohort random effects conditional modes from the base growth model using the best linear unbiased predictors (BLUP). We used BLUPs of the year random effects as the Annual Growth Index—a biochronology indicating years of above and below-average growth for each population. The linear mixed-effects models were developed in *R* (R Core Team, 2020) using the *lme4* package (Bates et al., 2015).

Synchrony Index (Syndex) within populations and age groups

Unlike other growth chronology studies, our focus was not on growth synchrony among populations, but on the

degree to which individuals from a given cohort of fish differ (or are synchronous) in their annual growth. We focused on three clear indices of within-cohort, within-age annual growth variability: the SD of the raw otolith increment widths, the coefficient of variation (CV) of the raw otolith increment widths, and the residuals from a base growth model (“Syndex,” described below). All three indices provided similar analytical results in the models, and all three indices were highly correlated among each other (Appendix S1: Figure S2). However, the residuals from a base growth model had the advantage of eliminating variability and artifacts due to individual variations in otolith transect length or initial growth rate (the random effect due to fish ID). Thus, the Syndex was calculated as the SD of the residuals extracted from the base growth model (see above) for a given population, year and age group, subsequently inverted for easier interpretation. There was negligible temporal autocorrelation in the base growth model residuals ($AR1 = 0.011$). The Syndex is inversely proportional to the variance remaining after accounting for the population-specific age-dependent decline in growth rate, and for mean differences in growth between years and cohorts, while allowing for individual growth trajectories. Thus, a high value of the Syndex indicates higher intra-annual growth synchrony among individuals, that is, all individuals are growing the same way, after accounting for systematic differences among years, cohorts, and individuals.

Modeling of Syndex

In the preliminary phase, we tested the relationships between Syndex and SST, EOF-1, EOF-2, water temperature at depth, age-specific growth rate, bivalve growth, zooplankton abundance, and cod stock abundance at age using simple linear models fitted separately for each age group and population. EOF-2, age-specific growth rate, and cod stock abundance were selected for further modeling as they appeared to show effects on Syndex. The relationships between the Syndex and the selected environmental variables were assessed with linear mixed-effect models using the following formula:

$$y_{ijk} = \alpha_i + \alpha_j \times f(\cdot) + \alpha_k^Y + \varepsilon_{ijk}$$

$$\alpha_k^Y \sim N(0, \sigma_Y^2), \quad \varepsilon_{ijk} \sim N(0, \sigma^2)$$

where y_{ijk} is Syndex y for population i and age group j at year k , α_i is the overall intercept for population i , α_j is the intercept for age group j , α_k^Y is the random intercept for year k , $f(\cdot)$ indicates environmental effects and their

interactions with age group j . Models were fitted using the number of observations (measurements of annual increment width) as a weight in the model fitting process (Bates et al., 2015). Due to limited availability of stock size data for some populations, we conducted two series of AIC_c -based model comparisons and selected two optimal models explaining the variability of the Syndex. Firstly, we included all five populations in the global model with EOF2 and the BLUPs (annual growth index) as predictors (Model 1). Secondly, we included only the three populations with accurate abundance at age data (i.e., Iceland [ICE], Norway [NOR], Faroese [FAR]) in the global model with EOF2, BLUPs, and scaled stock size as predictors (Model 2). We selected the optimal model structure (which has the best predictive accuracy) using marginal AIC_c values (Aho et al., 2014; Burnham & Anderson, 2007). For the selection, we used the *dredge* function of MuMIn package, which generates a set of models with combinations (subsets) of fixed effect terms from the global model (Bartoń, 2019). We obtained the predicted effects of the explanatory variables included in the selected optimal models using the effects package (Fox & Weisberg, 2019). The linear mixed-effects models were developed in R (R Core Team, 2020) using the *lme4* package (Bates et al., 2015).

RESULTS AND DISCUSSION

Temperature, food supply, and cohort abundance are the most influential variables controlling the indeterminate growth patterns of fish and other poikilotherms. In species such as cod, which can reach an age of 25 years, these variables are strongly entangled within age-structured population dynamics (Brander, 2010). In this study, we reconstructed up to 86 years of fish growth using measurements of 74,662 annual growth increments recorded in otoliths of 13,749 cod, sampled across five discrete cod populations spanning nearly the entire species range in the Northeast Atlantic (Figure 1; Appendix S1: Table S1). Traditional growth biochronology studies are often focused on climate reconstruction, and thus are designed to maximize signal: noise ratios through the careful selection of relatively few, long-lived individuals with well-resolved growth increments. Cohort effects (year of “birth”) on growth, a more ecological question, are generally not considered (Brienen et al., 2017). The strong effects of cohort abundance and density-dependent controls on fish growth require much greater sample depth across ages and cohorts to resolve the relative importance of the different growth drivers. Therefore, the effects of age, individual, cohort, and date of increment formation in each fish’s growth sequence were disentangled using

mixed-effects models and large annual sample sizes across ~80 year-classes (cohorts) per population (Morrongiello & Thresher, 2015).

Strong temporal and spatial coherence in cod growth-at-age was both expected and observed (Figure 2), with annual age-specific growth (estimated by best linear unbiased predictions [BLUPs] from Model 1 in Appendix S1: Table S2) often positively correlated with SST (Appendix S1: Figure S1). Although not previously reported over the centennial time scales reported here, ocean basin-wide synchrony in cod recruitment and productivity has been documented before (Brander, 2010) and was not a primary focus of our study. Of greater interest was the extent of growth synchrony among individuals within a given cohort, age group and population, as quantified with the inverse of the SD of the residuals of Model 1 (the Synchrony Index or “Syndex”).

A high value of the Syndex indicates that all individuals in the year and cohort grew at similar rates, be that fast or slow (Figure 1a). Both the SD and the CV of the raw otolith increment widths were highly correlated with the Syndex within a given age group, year and population (Appendix S1: Figure S2), indicating that all provided similar measures of intra-cohort growth variation, although only the Syndex accounted for systematic differences among years, cohorts, and individuals. Over the time span of the study, growth BLUPs (representing a proxy for interannual variation in average growth across individuals) and the Syndex were moderately correlated, although periods of high growth synchrony were evident in years where growth rate was either high or low (Appendix S1: Figure S3). Nonetheless, decadal

scale periodicity was clearly evident in the age- and population-specific Syndex values (Figure 3), suggesting that an external forcing variable linked with climate could play a role in driving growth synchrony within a cohort of a population.

To provide a more synoptic view of climate across our study area in the NE Atlantic, an empirical orthogonal function (EOF) was applied to the May through October mean SST data, resulting in two components accounting for 61% of the variance (Appendix S1: Figure S4). EOF-1 (45% of the variance) was interpreted as a direct proxy of SST over the study region, and was correlated with the Atlantic Multidecadal Oscillation ($r = -0.59$; 1948–2020). The overall relationship between EOF-1 and EOF-2 (16% of the variance) appears to be similar to that between the North Atlantic Oscillation (NAO) and the East Atlantic Pattern (EAP), these being the leading modes of atmospheric variability in the North Atlantic (Iglesias et al., 2014; Mellado-Cano et al., 2019). Since EOF-1 was not significantly correlated with the Syndex in any of the populations ($p > 0.05$), it was not considered further in any analyses. In contrast, EOF-2 was strongly collinear with the age- and population-specific synchrony indices in all of the cod populations (Figure 3a–d). Variation in the wind stress curl anomaly associated with the EAP can cause the polar front to retreat westward and allow the northward advection of more saline subtropical waters (Häkkinen et al., 2011). This dynamic may provide the link between the EAP, EOF-2, and our Syndex (Appendix S1: Figure S5). The EOF-2 time series also tracked 150 years of *Arctica islandica* bivalve growth anomalies off of south

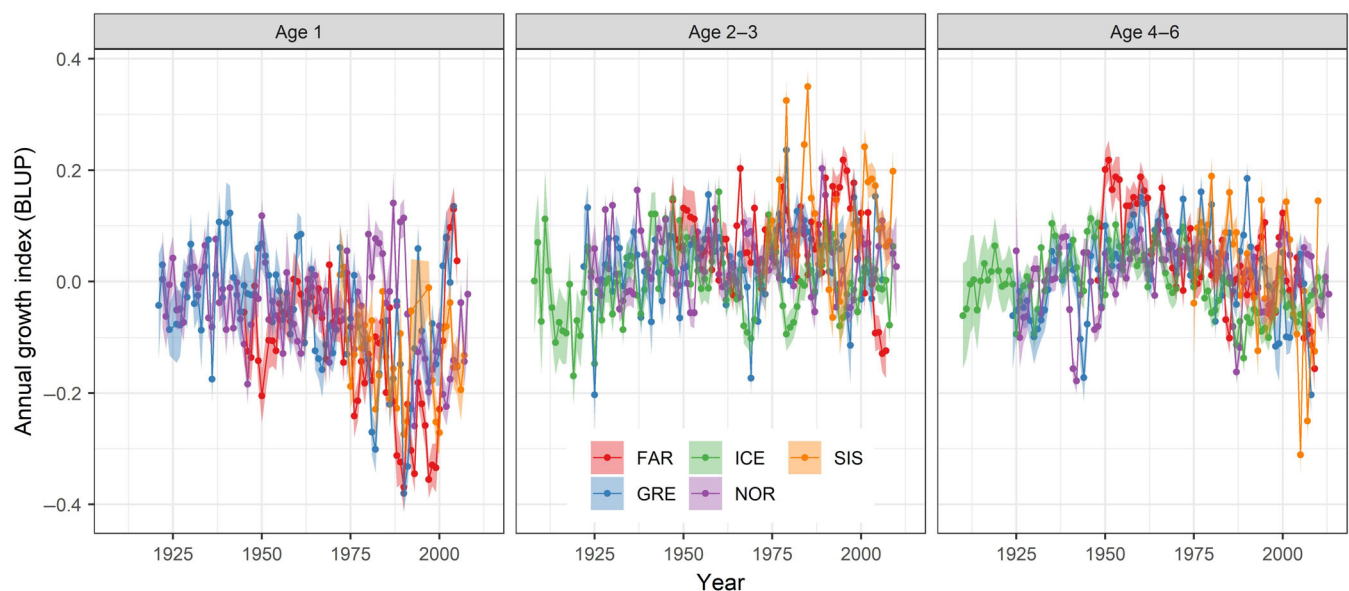


FIGURE 2 Annual growth indices for each cod age group (BLUPs ± standard error [SE]), adjusted for random effects of individual fish, color-coded by cod population.

Iceland ($r = 0.37$, $df = 69$, $p = 0.002$, Figure 3e) suggesting that EOF-2 reflected other oceanic variables such as stratification and nutrient supply more than SST. The much longer history provided by *Arctica* biochronologies from the southern Barents Sea suggests that EOF-2 has been characterized by low-frequency, multidecadal variability over at least the past 500 years (Mette et al., 2021).

A suite of hierarchical mixed-effects models was developed to identify the variables that could be driving Syndex fluctuations. These models included combinations of SST, EOF-2, water temperature at depth, age-specific growth rate, bivalve growth, and zooplankton abundance, while controlling for population, age group, year, cohort, and individual effects. Density dependence was considered in a later set of models for the subset of populations where

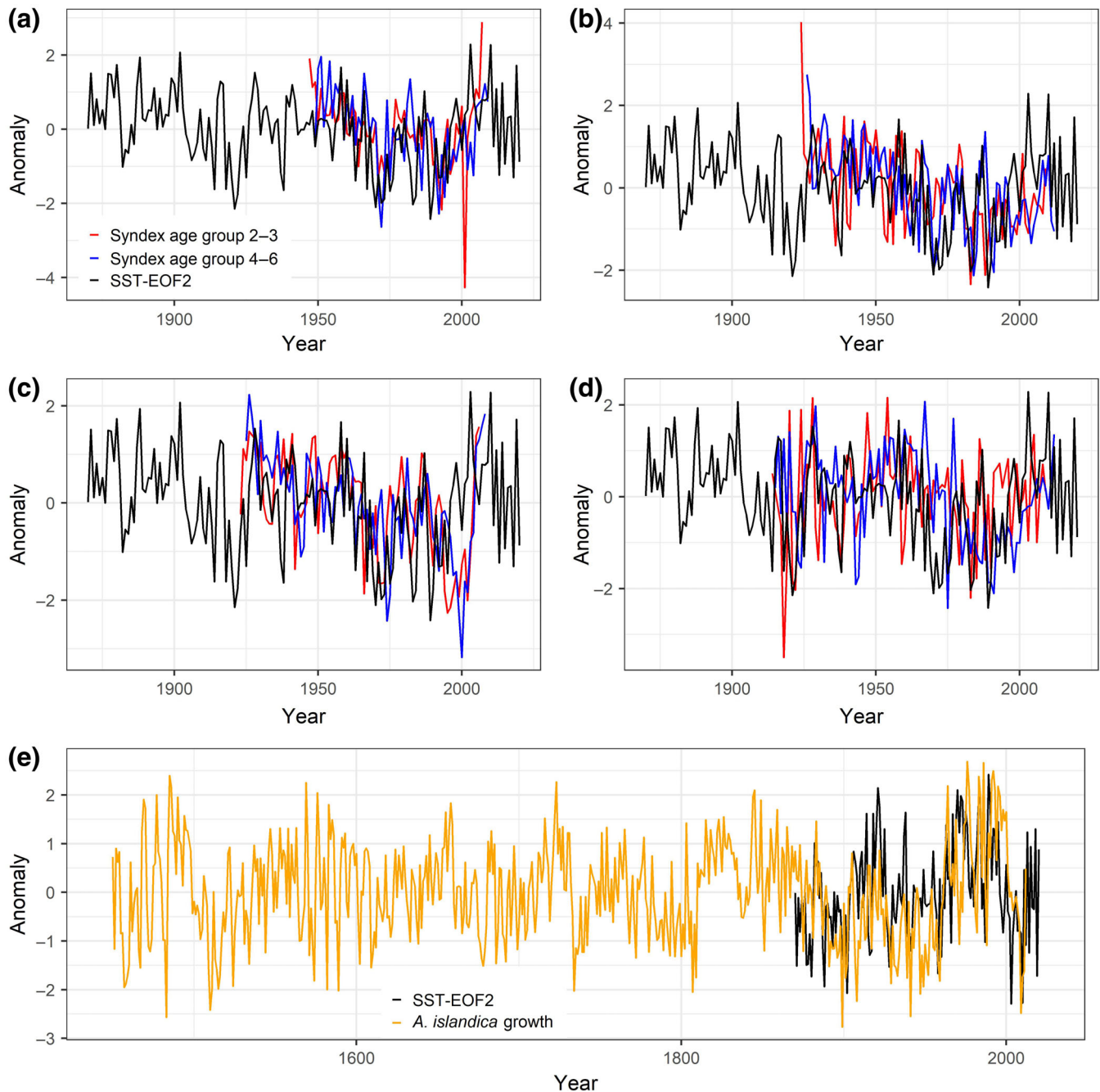


FIGURE 3 Time series of EOF-2 (second empirical orthogonal function of sea surface temperature) overlaid on the age-specific growth synchrony index (Syndex) for cod stocks in the Faroe Islands, FAR (a), Norway, NOR (b), Greenland, GRE (c) and Iceland, ICE (d). The detrended Norwegian bivalve (*Arctica islandica*) growth chronology (Mette et al., 2021) (e) shows growth anomalies relative to long-term mean growth, rather than synchrony. EOF2 in (e) is inverted.

the data were available. The optimal model (Model 1), based on AIC_c , included only age-specific growth rate (slope = 0.054, SE = 0.014) and EOF-2 (slope = 0.053, SE = 0.013) as covariates (Appendix S1: Table S2). The Syndex was predicted to increase by 6%–30% over the range of the growth rate BLUPs, and to increase by 2%–18% over the observed range of EOF-2 values (Figure 4). Similar trends were observed in a model incorporating SST rather than EOF-2 (Appendix S1: Figure S6). There are no previous reports of changes in age- and cohort-specific growth synchrony in fishes due to large-scale climate phenomena. However, our results suggest that increases in among-individual growth synchrony can be expected in cod population cohorts as either average growth rates or EOF-2 increases.

Density dependence has a strong effect on fish growth, whereby abundant cohorts grow more slowly than would otherwise be expected (Whitten et al., 2013). However, there is no obvious reason why intra-cohort growth should become increasingly synchronized as abundance increases. Mixed-effects models of the three cod populations with accurate abundance-at-age data (Icelandic, Faroese, and Norwegian/Northeast Arctic) resulted in a final model (Model 2) with age-specific growth rate, EOF-2 and scaled population abundance as covariates, based on AIC_c (Appendix S1: Table S3). As with Model 1, the Syndex increased linearly with growth rate (slope = 0.032, SE = 0.018) and EOF-2 (slope = 0.045, SE = 0.011), but Syndex also increased logarithmically with scaled population abundance (Figure 5). The magnitude of the EOF-2 effect on Syndex was similar in the models with and without population abundance, but the magnitude of the age-specific growth rate effect was reduced by about 40% in Model 2, presumably due to the countervailing effect of reduced growth at high stock abundance. Given the varied magnitudes and time series of fishing mortality in the

three populations, there is no obvious effect of fishing on Syndex except through its impact on abundance.

Cod is a broadly distributed, eurythermic species in the North Atlantic (Righton et al., 2010) but would not normally be considered representative of the pelagic or deep-sea environment. To test the generality of our findings in other environments, the growth chronology data underlying published results in five additional Northeast Atlantic fish species were re-analyzed for evidence of unreported intra-cohort growth synchrony. A positive relationship between Syndex and EOF-2 (slope = 0.043, SE = 0.013) was detected in the pelagic fish species, Atlantic horse mackerel (*Trachurus trachurus*), collected off the Portuguese coast, an effect that remained when population abundance was included in the model (slope = 0.031, SE = 0.006) (Appendix S1: Table S4). The effect of age-specific growth rate on Syndex in the optimal model was negative (slope = -0.146, SE = 0.047). Positive Syndex-EOF-2 relationships (slopes ranging between 0.015 and 0.033) were also identified in European hake from the Iberian coast, *Merluccius merluccius*, and in North Sea plaice, *Pleuronectes platessa*, as well as two deep-sea scorpaenid fishes (blackbelly rosefish, *Helicolenus dactylopterus* and offshore rockfish *Pontinus kuhlii*) from the Azores, but these relationships were not included in the optimal model (Appendix S1: Table S4). While the EOF-2 effects in these other species were not significant, rendering any conclusions somewhat tentative, the value of their slopes was consistent with those observed in cod. The statistical power of Model 1 to detect EOF-2 effects on Syndex in cod was 92%. Assuming the same magnitude of effect in a simplified model of the other species (where sample depth was less than 16% of that of cod), the power to detect this effect in the other species would only be 16%–40%. Clearly, a longer and more heavily sampled time series (sample depth > 350) would have been required to

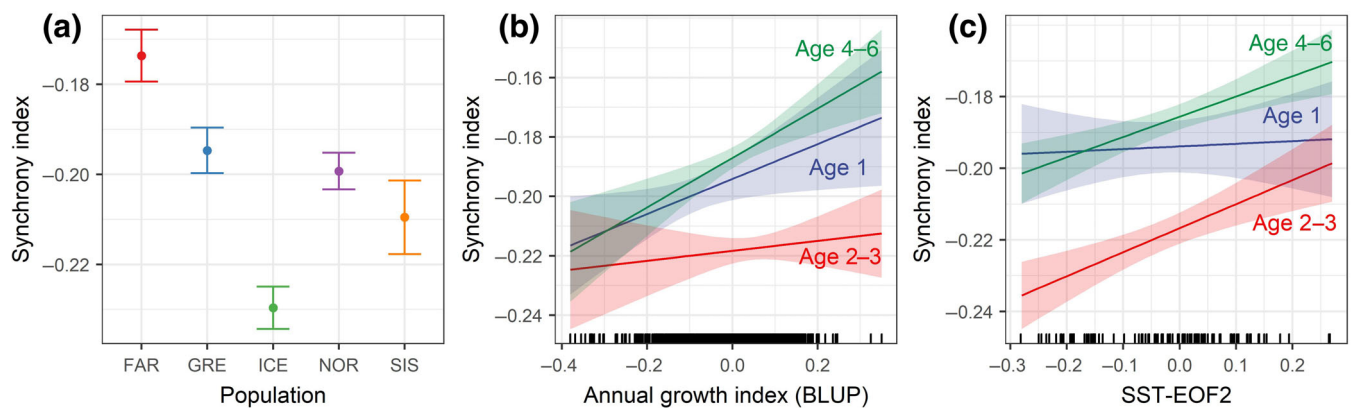


FIGURE 4 Predicted effects of factors in the final model of the Growth Synchrony Index (Syndex) as a function of (a) population, (b) mean growth by age group, and (c) empirical orthogonal function (EOF2) by age group (described in Appendix S1: Table S2). Shaded bands and error bars depict 95% confidence interval.

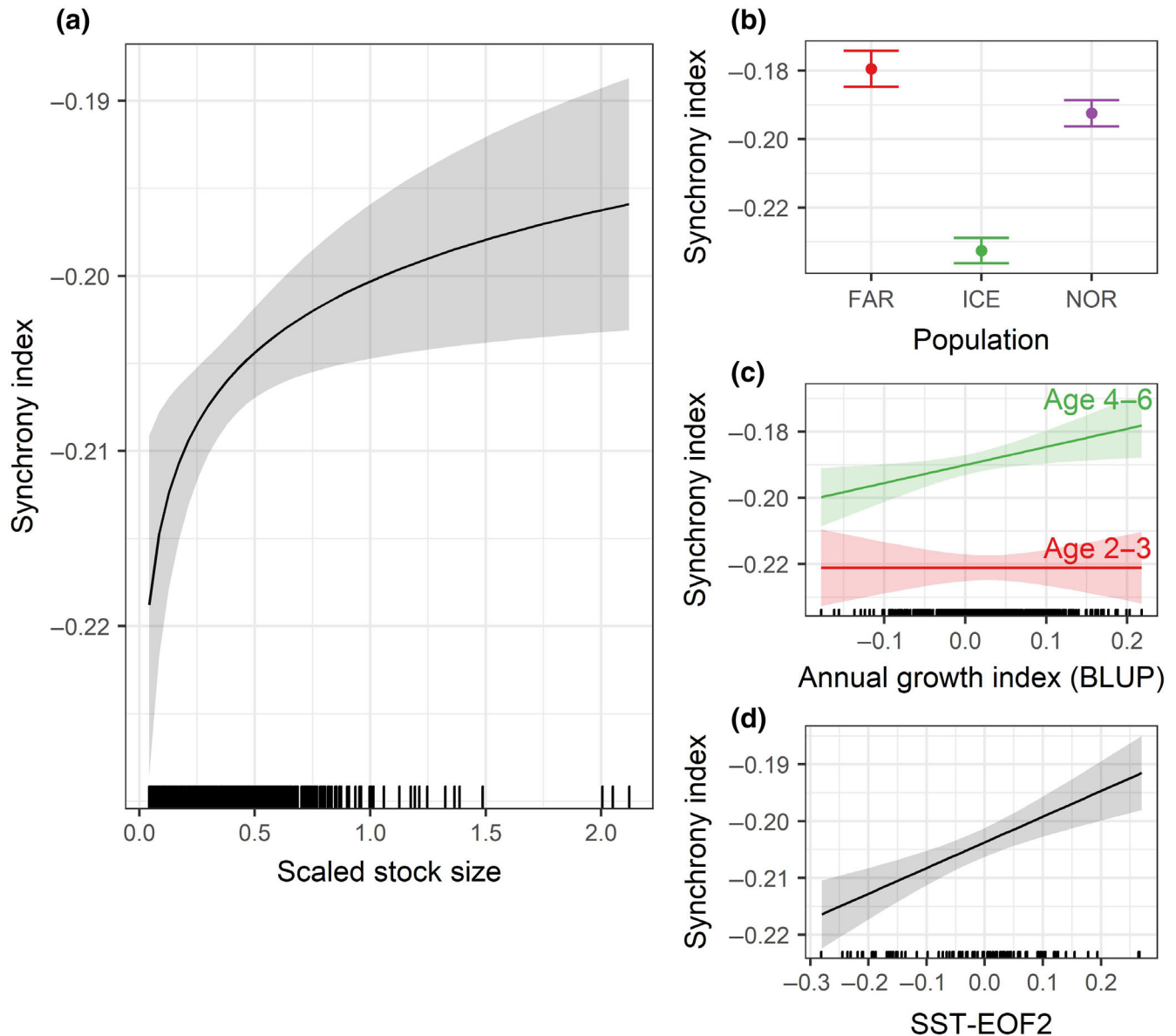


FIGURE 5 Predicted effects of factors in the final model of the Growth Synchrony Index (Syndex) as a function of (a) scaled population abundance, (b) population, (c) mean growth by age group, and (d) empirical orthogonal function (EOF)-2 (described in Appendix S1: Table S3). Only those populations for which abundance data were available were fit to the model. Shaded bands and error bars depict 95% confidence interval. BLUP, best linear unbiased predictors; SST, sea surface temperature.

detect the climate-growth synchrony effect in the other species we examined.

Growth chronologies from existing bivalve and tree rings (Black, 2009) are a resource for further exploring patterns of synchrony among individuals and comparing them to our results from Atlantic cod. We selected two examples of unfiltered bivalve and tree chronologies for further analysis: a bivalve (*Arctica islandica*) chronology from southern Iceland and tree ring growth measurement time series from a site in Scandinavia. The residual variance from bivalve (*Arctica islandica*) measurement time series from southern Iceland was strongly influenced by ontogenetic growth changes at early life stages, so

samples were restricted to eight individuals that settled before 1870. Analyses of growth synchrony showed a negative effect of average growth rate on Syndex (slope = -0.076 , SE = 0.025 ; Appendix S1: Table S5). The relationship with EOF-2 was positive but not supported with the AIC_c (slope = 0.094 , SE = 0.072), with a statistical power to detect an EOF effect of 41%. A parallel analysis of 29 long-term Scandinavian tree ring growth measurement time series, similarly filtered to include only trees germinated before 1870, revealed effects of both average growth (slope = -0.222 , SE = 0.020) and EOF-2 (slope = 0.095 , SE = 0.047 ; Appendix S1: Table S6). The negative relationship between average growth and growth

synchrony observed in both the bivalves and trees is opposite to that observed in cod, and is consistent with expectations that poor growth years would impose reduced growth equally and synchronously on individuals if they are unable to move to escape deleterious conditions (Ranta et al., 1997). While recognizing the low sample sizes associated with the tree and bivalve analyses, the remaining effect of EOF-2 was consistent with that identified in all the fish species, suggesting a common climatic influence.

A causative mechanism for the growth synchronization effect described here is not as readily explained as the more commonly considered direct effect of water temperature and other climate variables on average growth rate. In gape-limited animals such as fish, size, and growth divergence within a cohort is common and occurs as increasing density and intraspecific competition limit resources that in turn drive larger individuals to undertake size-dependent dietary shifts (Pfister & Stevens, 2002; Ratcliffe et al., 2018). Conversely, compensatory growth leading to size convergence has previously been noted in amphibians (Asquith & Vonesh, 2012) and in fish aggregations where there has been a competitive release following a reduction in population density (Ali et al., 2003). However, population-level synchronized growth responses like those documented here would appear to require either reduced intra-specific competition (Huss et al., 2008) or be the product of a narrowing initial size distribution caused by a reduced temporal width of hatching or recruitment windows (Heermann et al., 2017). Neither of these processes seem likely to simultaneously operate at the multi-population scale observed here, given the differences in relative abundance among the populations.

In a series of experiments evaluating the effect of natural selection on growth rate and fitness (Carlson et al., 2004), the authors concluded that compensatory growth of small individuals could only proceed if the survival cost was low, which occurred most often when population growth rates were fastest and density-dependent habitat selection was size-structured. Increased growth rates associated with range extensions would appear to be one mechanism through which this might occur, but these have not been observed in our study populations. An alternative possibility is that the increased growth variability in poor years reflects the inability of some individuals to adequately respond to a resource-poor environment (i.e., a constraint rather than adaptive variation). However, such a mechanism does not adequately explain the increased growth synchrony in good years, when enhanced competition that drives growth divergence might otherwise be expected. Although a defining mechanism driving the intra-cohort growth

synchronization remains unclear, the presence of a negative growth-synchrony relationship in immobile trees and bivalves, where competitive relationships differ so clearly from those in mobile fishes, supports the involvement of competition in the synchrony effect. Further research may clarify this issue.

The destabilizing effects of synchronized productivity across multiple populations are well documented (Schindler et al., 2010). Synchronized abundance or recruitment trends can render broad regions or entire species more prone to extirpation in the event of a deleterious climate event, since there are no nearby populations remaining to re-stock the failed groups. However, the ecological effects of synchronized growth trends at the level of individuals are poorly understood. Our results indicate that individuals from a given cohort and population which are exposed to a single large-scale climatic event are not necessarily all tied to the same fate: although intra-cohort growth was more synchronized during good years when a narrow growth portfolio would favor population health, growth asynchrony developed during poor growth years thus producing a diverse portfolio which could be more capable of buffering the population from the poor environmental conditions. Under this hypothesis, desynchronized growth within a cohort would extend the maturation schedule of that cohort and could conceivably reduce the impact of size-selective predation on a small, and thus more vulnerable, cohort. Thus, periods of high among-individual synchrony would reflect trait optimization and periods of low synchrony would reflect diversified bet hedging, both of which can be viewed as adaptive but plastic responses to the environment. Delayed maturation in harsher or more variable environments has previously been implicated as a diversified bet hedging mechanism, both theoretically and empirically (Cohen, 1966; Morrongiello, Bond, et al., 2012; Morrongiello, Thresher, & Smith, 2012). The capacity to respond rapidly to changing environmental conditions may be particularly important to relatively short-lived poikilothermic organisms such as fish and would be most readily provided with labile traits such as growth (Smoliński, Deplanque-Lasserre, et al., 2020).

Population-specific spawning windows and shifts in size-at-maturity caused by differences in within-cohort growth are well documented in fish populations (Hutchings & Myers, 1993). An alternative, non-adaptive explanation postulates that observed declines in growth synchrony in poor growth years are caused by only some individuals having access to resources. While this is plausible, it is contradicted by the increased synchrony observed in high abundance years, which would appear incompatible with a higher competition for resources and thus a greater potential for “winners and losers”. Further work to explore the adaptive benefit of diversified

fish size at maturity and subsequent impacts on vulnerability to size-dependent predation would be fruitful. Notably however, there was no evidence to suggest that growth asynchrony could form the basis for an evolutionary response to climate change. The absence of a positive growth effect on synchrony in the bivalves and trees would then be consistent with the reduced importance of short-term fluctuations in growth rate for the fitness and survival of long-lived bivalves and trees (Russo et al., 2021).

Climate change is routinely painted as inducing irreversible negative effects, with species and populations as hapless victims, yet adaptations to climate change have evolved at both the individual and population level (Crozier & Hutchings, 2014). Through the plasticity of growth, intra-cohort growth synchronization in fish may serve as a rapidly responding yet influential evolutionary buffer to a variable environment. The multi-decadal periodicity of the East Atlantic Pattern (EOF-2), which lacks the directional component of climate change evident in SST, and which produced a neutral effect on growth synchrony over the long term, is consistent with this interplay between growth synchronization and climate change.

ACKNOWLEDGMENTS

This work was supported by Icelandic Research Fund (RANNIS) Grant 173906-051 to Steven E. Campana. Gotje von Leesen also received support from The Eimskip University Fund (project number: 1535-1533127). Szymon Smoliński and Côme Denechaud received additional support from the Institute of Marine Research (Project No. 14260). Madelyn Mette was hosted by NORCE Norwegian Research Centre. Peter Grønkvær received funding from the Nordic Council of Ministers (project No. 25014.17). Susanne E. Tanner was supported by Fundação para a Ciência e a Tecnologia (FCT) through CEECIND/02710/2021, UIDB/04292/2020 and LA/P/0069/2020. John R. Morrongiello was supported by the Australian Research Council (DP190101627) and the Australian Academy of Science's Thomas Davies Research Grant. Carin Andersson received additional funding from the Research Council of Norway project 240550. Audrey J. Geffen was supported by the Department of Biological Sciences, University of Bergen and the Nordic Council of Ministers (project No. 25014.17). Any use of trade, product, or firm names is for descriptive purposes only and does not imply endorsement by the U.S. Government.

CONFLICT OF INTEREST

The authors declare no conflict of interest.

DATA AVAILABILITY STATEMENT

Data (Campana, 2022a) are available in Dryad at <https://doi.org/10.5061/dryad.t4b8gtj4s>. Code for the Syndex calculation is not novel, but is provided in Zenodo at <https://doi.org/10.5281/zenodo.6792729> (Campana, 2022b) for ease of use.


ORCID

Steven E. Campana  <https://orcid.org/0000-0002-7453-3761>

Szymon Smoliński  <https://orcid.org/0000-0003-2715-984X>

Bryan A. Black  <https://orcid.org/0000-0001-6851-257X>

John R. Morrongiello  <https://orcid.org/0000-0002-9608-4151>

Carin Andersson  <https://orcid.org/0000-0002-7113-6066>

Bjarte Bogstad  <https://orcid.org/0000-0002-6630-8994>

Paul G. Butler  <https://orcid.org/0000-0002-9924-0316>

Côme Denechaud  <https://orcid.org/0000-0002-8298-4423>

David C. Frank  <https://orcid.org/0000-0001-5463-5640>

Audrey J. Geffen  <https://orcid.org/0000-0002-6946-5282>

Jane Aanestad Godiksen  <https://orcid.org/0000-0001-5491-2433>

Peter Grønkvær  <https://orcid.org/0000-0003-1337-4661>

Ingibjörg G. Jónsdóttir  <https://orcid.org/0000-0001-9329-7410>

Mark Meekan  <https://orcid.org/0000-0002-3067-9427>

Madelyn Mette  <https://orcid.org/0000-0002-4504-8847>

Susanne E. Tanner  <https://orcid.org/0000-0003-2225-7002>

Gotje von Leesen  <https://orcid.org/0000-0003-1795-9413>

REFERENCES

- Aho, K., D. Derryberry, and T. Peterson. 2014. "Model Selection for Ecologists: The Worldviews of AIC and BIC." *Ecology* 95(3): 631–6.
- Ali, M., A. Nicieza, and R. J. Wootton. 2003. "Compensatory Growth in Fishes: A Response to Growth Depression." *Fish and Fisheries* 4(2): 147–90.
- Asquith, C. M., and J. R. Vonesh. 2012. "Effects of Size and Size Structure on Predation and Inter-Cohort Competition in Red-Eyed Treefrog Tadpoles." *Oecologia* 170(3): 629–39.
- Bartoń, K. 2019. "Package MuMIn: Multi-Model Inference." <http://R-Forge.R-project.org/projects/mumin>.
- Bates, D., M. Mächler, B. M. Bolker, and S. C. Walker. 2015. "Fitting Linear Mixed-Effects Models Using lme4." *Journal of Statistical Software* 67(1): 1–48.
- Beaugrand, G., K. M. Brander, J. A. Lindley, S. Souissi, and P. C. Reid. 2003. "Plankton Effect on Cod Recruitment in the North Sea." *Nature* 426(6967): 661–4.
- Beaugrand, G., and R. R. Kirby. 2010. "Climate, Plankton and Cod." *Global Change Biology* 16(4): 1268–80.

- Beverton, R. J. H., and S. J. Holt. 1957. *On the Dynamics of Exploited Fish Populations*. Fishery Investigations Ser. 2, Vol 19. London: Her Majesty's Stationery Office.
- Black, B. A. 2009. "Climate-Driven Synchrony across Tree, Bivalve, and Rockfish Growth-Increment Chronologies of the Northeast Pacific." *Marine Ecology Progress Series* 378: 37–46.
- Black, B. A., P. van der Sleen, E. Di Lorenzo, D. Griffin, W. J. Sydeman, J. B. Dunham, R. R. Rykaczewski, et al. 2018. "Rising Synchrony Controls Western North American Ecosystems." *Global Change Biology* 24(6): 2305–14.
- Brander, K. M. 2010. "Cod *Gadus morhua* and Climate Change: Processes, Productivity and Prediction." *Journal of Fish Biology* 77(8): 1899–911.
- Brienen, R. J. W., M. Gloor, and G. Ziv. 2017. "Tree Demography Dominates Long-Term Growth Trends Inferred from Tree Rings." *Global Change Biology* 23(2): 474–84.
- Burnham, K. P., and D. Anderson. 2007. *Model Selection and Multimodel Inference: A Practical Information-Theoretic Approach*. New York, NY: Springer.
- Campana, S. 2022a. "Otolith Annual Growth Increments for Cod Populations in the Northeast Atlantic." Dryad, Dataset. <https://doi.org/10.5061/dryad.4tb8gtj4s>.
- Campana, S. 2022b. "Otolith Annual Growth Increments for Cod Populations in the Northeast Atlantic." Zenodo. <https://doi.org/10.5281/zenodo.6792729>.
- Campana, S. E. 2001. "Accuracy, Precision and Quality Control in Age Determination, Including a Review of the Use and Abuse of Age Validation Methods." *Journal of Fish Biology* 59: 197–242.
- Carlson, S. M., A. P. Hendry, and B. H. Letcher. 2004. "Natural Selection Acting on Body Size, Growth Rate and Compensatory Growth: An Empirical Test in a Wild Trout Population." *Evolutionary Ecology Research* 6: 955–73.
- Christensen, J. M. 1964. "Burning of Otoliths, a Technique for Age Determination of Soles and Other Fish." *ICES Journal of Marine Science* 29(1): 73–81.
- Cohen, D. 1966. "Optimizing Reproduction in a Randomly Varying Environment." *Journal of Theoretical Biology* 12(1): 119–29.
- Cook, E. R., P. J. Krusic, K. Peters, and R. L. Holmes. 2017. *Program ARSTAN (Version 48d2): Autoregressive Tree-Ring Standardization Program*. Palisades, NY: Tree-Ring Laboratory of Lamont–Doherty Earth Observatory.
- Crozier, L. G., and J. A. Hutchings. 2014. "Plastic and Evolutionary Responses to Climate Change in Fish." *Evolutionary Applications* 7(1): 68–87.
- Denechaud, C., S. Smoliński, A. J. Geffen, J. A. Godiksen, and S. E. Campana. 2020. "A Century of Fish Growth in Relation to Climate Change, Population Dynamics and Exploitation." *Global Change Biology* 26(10): 5661–78.
- Dettman, D. L., A. K. Reische, and K. C. Lohmann. 1999. "Controls on the Stable Isotope Composition of Seasonal Growth Bands in Aragonitic Fresh-Water Bivalves (Unionidae)." *Geochimica et Cosmochimica Acta* 63(7/8): 1049–57.
- Dmitriew, C. M. 2011. "The Evolution of Growth Trajectories: What Limits Growth Rate?" *Biological Reviews* 86(1): 97–116.
- Fox, J., and S. Weisberg. 2019. *An R Companion to Applied Regression*, 3rd ed. Thousand Oaks, CA: Sage Publications, Inc.
- Grossman, E. L., and T.-L. Ku. 1986. "Oxygen and Carbon Isotope Fractionation in Biogenic Aragonite: Temperature Effects." *Chemical Geology: Isotope Geoscience* 59: 59–74.
- Häkkinen, S., P. B. Rhines, and D. L. Worthen. 2011. "Warm and Saline Events Embedded in the Meridional Circulation of the Northern North Atlantic." *Journal of Geophysical Research: Oceans* 116(C3): C03006.
- Hansen, P. M., A. S. Jensen, and Å. W. Tåning. 1935. "Cod Marking Experiments in the Waters of Greenland, 1924–1933." In *Meddelelser fra Kommissionen for Danmarks Fiskeri- og Havundersøgelser. Serie: Fiskeri*, Vol 10. Copenhagen: Reitzel.
- Heermann, L., D. L. DeAngelis, and J. Borchering. 2017. "A New Mechanistic Approach for the Further Development of a Population with Established Size Bimodality." *PLoS One* 12(6): e0179339. <https://doi.org/10.1371/journal.pone.0179339>.
- Helaouet, P. 2020. "Marine Biological Association of the UK (MBA) CPR Data Request Stella Alexandroff Exeter University July 2020." Distributed by the Archive for Marine Species and Habitats Data (DASSH). <https://doi.org/10.17031/1652>.
- Huss, M., P. Byström, and L. Persson. 2008. "Resource Heterogeneity, Diet Shifts and Intra-Cohort Competition: Effects on Size Divergence in YOY Fish." *Oecologia* 158(2): 249–57.
- Hutchings, J. A., and R. A. Myers. 1993. "Effect of Age on the Seasonality of Maturation and Spawning of Atlantic Cod, *Gadus morhua*, in the Northwest Atlantic." *Canadian Journal of Fisheries and Aquatic Sciences* 50: 2468–74.
- Hysten, A. 2002. "Fluctuations in Abundance of Northeast Arctic Cod during the 20th Century." *ICES Marine Science Symposia* 215: 543–50.
- ICES. 2019. "North-Western Working Group (NWWG)." *ICES Scientific Reports* 1: 14.
- ICES. 2020a. "Arctic Fisheries Working Group (AFWG)." *ICES Scientific Reports* 2: 52.
- ICES. 2020b. "North-Western Working Group (NWWG)." *ICES Scientific Reports* 2: 51.
- Iglesias, I., M. N. Lorenzo, and J. J. Taboada. 2014. "Seasonal Predictability of the East Atlantic Pattern from Sea Surface Temperatures." *PLoS One* 9(1): e86439. <https://doi.org/10.1371/journal.pone.0086439>.
- Kristiansen, A. 1988. "Results from the Groundfish Surveys at Faroes 1982–1988." *ICES CM* 1988/G:41.
- Liebold, A., W. D. Koenig, and O. N. Bjørnstad. 2004. "Spatial Synchrony in Population Dynamics." *Annual Review of Ecology, Evolution, and Systematics* 35: 467–90.
- Mellado-Cano, J., D. Barriopedro, R. García-Herrera, R. M. Trigo, and A. Hernández. 2019. "Examining the North Atlantic Oscillation, East Atlantic Pattern, and Jet Variability since 1685." *Journal of Climate* 32(19): 6285–98.
- Mette, M. J., A. D. Wanamaker, Jr., M. J. Retelle, M. L. Carroll, C. Andersson, and W. G. Ambrose, Jr. 2021. "Persistent Multidecadal Variability since the 15th Century in the Southern Barents Sea Derived from Annually Resolved Shell-Based Records." *Journal of Geophysical Research: Oceans* 126(6): e2020JC017074.
- Morrongiello, J. R., N. R. Bond, D. A. Crook, and B. B. M. Wong. 2012. "Spatial Variation in Egg Size and Egg Number Reflects Trade-Offs and Bet-Hedging in a Freshwater Fish." *Journal of Animal Ecology* 81: 806–17.
- Morrongiello, J. R., and R. E. Thresher. 2015. "A Statistical Framework to Explore Ontogenetic Growth Variation among Individuals and Populations: A Marine Fish Example." *Ecological Monographs* 85(1): 93–115.

- Morrongiello, J. R., R. E. Thresher, and D. C. Smith. 2012. "Aquatic Biochronologies and Climate Change." *Nature Climate Change* 2: 849–57.
- Pfister, C. A., and F. R. Stevens. 2002. "The Genesis of Size Variability in Plants and Animals." *Ecology* 83(1): 59–72.
- R Core Team. 2020. *R: A Language and Environment for Statistical Computing*. Vienna: R Foundation of Statistical Computing. <https://www.r-project.org>.
- Ranta, E., V. Kaitala, J. Lindström, and E. Helle. 1997. "The Moran Effect and Synchrony in Population Dynamics." *Oikos* 78(1): 136–42.
- Ratcliffe, N., S. Adlard, G. Stowasser, and R. McGill. 2018. "Dietary Divergence Is Associated with Increased Intra-Specific Competition in a Marine Predator." *Scientific Reports* 8: 6827. <https://doi.org/10.1038/s41598-018-25318-7>.
- Rayner, N. A., D. E. Parker, E. B. Horton, C. K. Folland, L. V. Alexander, D. P. Rowell, E. C. Kent, and A. Kaplan. 2003. "Global Analyses of Sea Surface Temperature, Sea ice, and Night Marine Air Temperature since the Late Nineteenth Century." *Journal of Geophysical Research* 108(D14): 4407.
- Righton, D. A., K. Haste Andersen, F. Neat, V. Thorsteinsson, P. Steingrund, H. Svedäng, K. Michalsen, et al. 2010. "Thermal Niche of Atlantic Cod *Gadus morhua*: Limits, Tolerance and Optima." *Marine Ecology Progress Series* 420: 1–13.
- Rørvik, C. J., B. Bogstad, G. Ottersen, and O. S. Kjesbu. 2022. "Long-Term Interplay between Harvest Regimes and Biophysical Conditions May Lead to Persistent Changes in Age-at-Sexual Maturity of Northeast Arctic Cod (*Gadus morhua*)." *Canadian Journal of Fisheries and Aquatic Sciences* 79(4): 576–86.
- Russo, S. E., S. M. McMahon, M. Detto, G. Ledder, S. J. Wright, R. S. Condit, S. J. Davies, et al. 2021. "The Interspecific Growth–Mortality Trade-off Is Not a General Framework for Tropical Forest Community Structure." *Nature Ecology and Evolution* 5(2): 174–83.
- Schindler, D. E., R. Hilborn, B. Chasco, C. P. Boatright, T. P. Quinn, L. A. Rogers, and M. S. Webster. 2010. "Population Diversity and the Portfolio Effect in an Exploited Species." *Nature* 465(7298): 609–12.
- Schopka, S. A. 1994. "Fluctuations in the Cod Stock off Iceland during the Twentieth Century in Relation to Changes in the Fisheries and Environment." *ICES Marine Science Symposia* 198: 175–93.
- Smoliński, S., J. Deplanque-Lasserre, E. Hjörleifsson, A. J. Geffen, J. A. Godiksen, and S. E. Campana. 2020. "Century-Long Cod Otolith Biochronology Reveals Individual Growth Plasticity in Response to Temperature." *Scientific Reports* 10: 16708. <https://doi.org/10.1038/s41598-020-73652-6>.
- Smoliński, S., J. Morrongiello, P. van der Sleen, B. A. Black, and S. E. Campana. 2020. "Potential Sources of Bias in the Climate Sensitivities of Fish Otolith Biochronologies." *Canadian Journal of Fisheries and Aquatic Sciences* 77(9): 1552–63.
- Stenseth, N. C., A. Mysterud, G. Ottersen, J. W. Hurrell, K.-S. Chan, and M. Lima. 2002. "Ecological Effects of Climate Fluctuations." *Science* 297(5585): 1292–6.
- Tanner, S. E., E. Giacomello, G. M. Menezes, A. Mirasole, J. Neves, V. Sequeira, R. P. Vasconcelos, A. R. Vieira, and J. R. Morrongiello. 2020. "Marine Regime Shifts Impact Synchrony of Deep-Sea Fish Growth in the Northeast Atlantic." *Oikos* 129(12): 1781–94.
- Tanner, S. E., A. R. Vieira, R. P. Vasconcelos, S. Dores, M. Azevedo, H. N. Cabral, and J. R. Morrongiello. 2019. "Regional Climate, Primary Productivity and Fish Biomass Drive Growth Variation and Population Resilience in a Small Pelagic Fish." *Ecological Indicators* 103: 530–41.
- Trouet, V., and G. J. van Oldenborgh. 2013. "KNMI Climate Explorer: A Web-Based Research Tool for High-Resolution Paleoclimatology." *Tree-Ring Research* 69(1): 3–13.
- van der Sleen, P., C. Stransky, J. R. Morrongiello, H. Haslob, M. Peharda, and B. A. Black. 2018. "Otolith Increments in European Plaice (*Pleuronectes platessa*) Reveal Temperature and Density-Dependent Effects on Growth." *ICES Journal of Marine Science* 75(5): 1655–63.
- Vieira, A. R., S. Dores, M. Azevedo, and S. E. Tanner. 2020. "Otolith Increment Width-Based Chronologies Disclose Temperature and Density-Dependent Effects on Demersal Fish Growth." *ICES Journal of Marine Science* 77(2): 633–44.
- von Leesen, G., B. Bogstad, E. Hjörleifsson, U. S. Ninnemann, and S. E. Campana. 2022. "Temperature Exposure in Cod Driven by Changes in Abundance." *Canadian Journal of Fisheries and Aquatic Sciences* 79(4): 587–600.
- von Leesen, G., U. S. Ninnemann, and S. E. Campana. 2020. "Stable Oxygen Isotope Reconstruction of Temperature Exposure of the Icelandic Cod (*Gadus morhua*) Stock over the Last 100 Years." *ICES Journal of Marine Science* 77(3): 942–52.
- Warner, A. J., and G. C. Hays. 1994. "Sampling by the Continuous Plankton Recorder Survey." *Progress in Oceanography* 34(2–3): 237–56.
- Weisberg, S., G. Spangler, and L. S. Richmond. 2010. "Mixed Effects Models for Fish Growth." *Canadian Journal of Fisheries and Aquatic Sciences* 67(2): 269–77.
- Whitten, A. R., N. L. Klaer, G. N. Tuck, and R. W. Day. 2013. "Accounting for Cohort-Specific Variable Growth in Fisheries Stock Assessments: A Case Study from South-Eastern Australia." *Fisheries Research* 142: 27–36.
- Wood, S. N. 2001. "Mgcv: GAMs and Generalized Ridge Regression for R." *R News* 1: 20–5.
- Wood, S. N. 2003. "Thin Plate Regression Splines." *Journal of the Royal Statistical Society. Series B: Statistical Methodology* 65: 95–114.

SUPPORTING INFORMATION

Additional supporting information can be found online in the Supporting Information section at the end of this article.

How to cite this article: Campana, Steven E., Szymon Smoliński, Bryan A. Black, John R. Morrongiello, Stella J. Alexandroff, Carin Andersson, Bjarte Bogstad, et al. 2023. "Growth Portfolios Buffer Climate-Linked Environmental Change in Marine Systems." *Ecology* 104(3): e3918. <https://doi.org/10.1002/ecy.3918>